The Reaction Cl + NO_2 → ClONO and $ClNO_2$†

David M. Golden

Department of Mechanical Engineering, Stanford University, Stanford, California 94305

Received: December 28, 2006; In Final Form: April 17, 2007

The extant data (see *Int. J. Chem. Kinet.* **1984**, *16*, 1311; *Int. J. Chem. Kinet.* **1988**, *20*, 811; and *J. Phys. Chem.* **1996**, *100*, 4019)[1−3] for the reaction of Cl atoms with NO_2 has been examined and compared with calculated values using RRKM/ME methods through the use of the coded suite "Multiwell" (see *Int. J. Chem. Kinet.* **2001**, *33*, 232; *MultiWell-2.08 Software*; University of Michigan: Ann Arbor, MI, 2007; http://aoss.engin.umich.edu/multiwell/)[4,5] and ab initio quantum calculations in the literature (see *J. Phys. Chem.* **1994**, *98*, 111; *J. Phys. Chem. A* **2005**, *109*, 4736; and *Chemphyschem* **2004**, *5*, 1864).[6−8] The data are in, or very near, the low-pressure limit and therefore sensitive to the density of states of the excited ClONO and $ClNO_2$ molecules as well as collisional energy transfer, centrifugal effects, and anharmonicity corrections. The data were underpredicted by a factor of 2.6 using accepted prescriptions for centrifugal corrections, collision frequency, and ignoring anharmonicity. The data could be fit by either making all rotational degrees of freedom active or artificially increasing the collision frequency, or maybe some of each. This last could also be complemented or supplemented by a multiplicative factor ascribed to anharmonicity.

1. Introduction

The reaction of chlorine atoms with nitrogen dioxide has been reported[9] to yield both ClONO, presumably in both cis and trans forms, and $ClNO_2$, with the former accounting for about 80% of the yield at temperatures around room temperature and pressures up to about one atmosphere. Chang et al.[10] seem to have explained the results quantitatively using Troe's low-pressure limit model,[11,12] and their results have been the basis for the values in the NASA/JPL[13] evaluation. Details can be found in Patrick and Golden (PG).[14] The Troe formalism would seem to treat systems with a significantly different view of the effect of rotational energy than found in standard books[15] and codes[4,5] employing RRKM theory. In fact, these different methods can be reconciled and give almost exactly the same results. (This is discussed in the Appendix.) Recently, two different studies[7,8] have presented potential energy surfaces for this system and this offered an opportunity to revisit the experiments employing the master equation code "Multiwell".[4,5] Both of these studies are in good agreement with respect to the structures, frequencies, and heats of formation of the stable species. They are also in agreement in these respects with the earlier study[6] of Lee. They are also in agreement on the structures, frequencies, and heats of formation of the transition state for cis−trans isomerization in ClONO. They differ substantially on the transition states for chlorine atom association with nitrogen dioxide to form *cis*- and *trans*-ClONO and $ClNO_2$.

In a recent study,[16] Multiwell was applied to the reaction IO + NO_2 and there was some difficulty in fitting the lowest pressure results without arguing that the species $IONO_2$ was more stable than reported. In unpublished work[17] on BrO + NO_2, the same problem has arisen. In that case, the heat of formation of $BrONO_2$ seems well-founded, so a bit of a conundrum remains. In contrast, application[18] of these standard methods to the reaction $H+CH_3=CH_4$ adequately describes the data over wide pressure and temperature ranges. For the title reaction, the data seem to be at, or very close to, the low-pressure limit, so it would seem that this offers a reasonable test system. These studies have been undertaken with the hope that the combined theoretical understanding of these systems, together with the experimental data that are often per force limited to accessible experimental regions, could be used to extrapolate data from the measured range to regions of parameter space of practical interest with some reasonable confidence. Thus, there is some imperative to understanding the aforementioned discrepancies.

2. RRKM/Master Equation Analysis

Because the data appear to be at or very close to the low-pressure limit, the full RRKM/ME analysis will not be very sensitive to the detailed nature of the transition state. However, because the transition states are located at or near the centrifugal barriers and these affect the energy available for the reaction, the procedure for taking this into account is detailed below. Also, it is of interest to confirm that the data in the measured regions are indeed in the low-pressure limit.

The analysis proceeded in the following fashion.

(i) Structures and frequencies for *cis*- and *trans*-ClONO and $ClNO_2$ were taken from either Sayin and McKee (SM)[7] or Zhu and Lin (ZL),[8] who often used values from Lee.[6] For the stable species and the cis−trans isomerization transition state, these are very similar. For these species the values from SM[7] were used. No conclusion reached herein is affected by any small differences among these studies.

(ii) Using the Cartesian coordinates in the Supporting Information in SM,[7] the values of the internuclear distance at the centrifugal maxima were computed. SM[7] also supplied coordinates for their relatively "tight" transition states for the association reactions, and moments of inertia were computed from these when comparing rate constants from that study to those computed herein.

There are several ways to compute the moments of inertia at the transition state. (a) In one method for the "loose" transition states, in keeping with earlier studies[19] in this series, and for

† Part of the special issue "M. C. Lin Festschrift".

10.1021/jp069000x CCC: $37.00
Published on Web 06/05/2007

similar "loose" transition states from the ZL[8] study, the moments of inertia can be computed as follows: The center of mass distance in the stable molecule was computed from the "*J* moment" by dividing by the reduced mass and taking the square root. The *J* moment is taken from the geometric mean of the two largest moments. Using a Morse potential, computed using this center of mass coordinate, the position of the centrifugal maximum was obtained by adding the rotational energy at the maximum, assumed (see page 64 of Holbrook et al.[15]) to be *kT*, and setting the derivative to zero. The Morse β parameter can be computed from the appropriate frequency and bond energy, $\beta = 2\pi c\omega(\mu/D_e)^{1/2}$, or from force constants given by Lee,[6] $\beta = (f/2D_e)^{1/2}$.

In fact, for $ClNO_2$, these both give exactly the same result. However, for ClONO, they differ. Furthermore, ZL[8] compute the approach of Cl and NO_2 to form ClONO and fit this to a Morse function. We have used their value, which is 10% lower than the value from Lee's[6] force constant. Unfortunately, ZL[8] do not give a value for Cl approaching NO_2 to yield $ClNO_2$. Using this method, values for the ratio of moments in the transition state (or activated species) $I^{\neq}/I$ are 5.79 ($ClNO_2$) and 3.65 (ClONO) at 300 K.

(b) Another method, which has been adopted here, uses formulas due to Troe[11,12] to compute the effective ratio of moments at the transition state to that of the stable molecule. These formulas require the calculation of the maxima as a function of the *J* quantum number, the centrifugal barriers. The formulas differ for linear and nonlinear species. Using the value for linear species, which applies here because the rotation around the figure axis, the "*K*-rotor", has been included in the density of states in the Multiwell calculation, values for the ratio of moments in the transition state (or activated species) $I^{\neq}/I$ are 5.38 ($ClNO_2$) and 3.43 (ClONO) at 300 K, almost identical to those above. (This will be discussed more thoroughly in the Appendix.)

Table 1, first section, contains the constants used and the value of the internuclear distance that results from the maximization of the potential at 300 K for both $ClNO_2$ and *cis*-ClONO. These values will change somewhat with values for the bond energy, but this effect was small enough in the 200−400 K temperature and ±2 kcal mol^{-1} bond energy range considered herein that the values were not varied. (Following SM,[7] the transition state for *trans*-ClONO is at high enough energy that it does not contribute.) These values can then be used to replace the Cl−NO_2 or Cl−ONO equilibrium bond length, and moments of inertia can be calculated for this new entity representing the structure at the centrifugal maximum.

Table 1, second section, shows the values of the centrifugal barriers computed at several values of *J*. These values were used to compute ratios of moments of inertia for the transition state and the stable molecule using equations due to Troe[12] given in the Appendix. Values computed by either method are quite similar. The values shown in Table 2 were from this method.

(iii) Frequencies and moments of inertia for the Gorin rotors in the transition state were those of NO_2 used previously.[19] The low-pressure limit and pressures close to this limit are not particularly sensitive to these values.

(iv) Energy transfer with the nitrogen bath gas was computed using the exponential down probability function, and the value of $\langle\Delta E\rangle_{down}$ could be adjusted in an attempt to reproduce experiment. In fact, there are sufficient uncertainties in so many input parameters that only computations using 500 cm^{-1} as the value of $\langle\Delta E\rangle_{down}$ are reported. Lennard−Jones collision parameters and the value of $\langle\Delta E\rangle_{down}$ are given in Table 2.

(v) Because all of the data are in, or very close to, the low-pressure limit, the NASA/JPL[13] values for the high-pressure limit are little more than estimates. Hindrance values of 0% (full Gorin model) were chosen as a starting point, and there is little reason to get more detailed. Because the output of the Multiwell code[4,5] used for the calculations is the fraction of dissociation, $k_{diss}(P,T)/k_{diss,\infty}(T)$ and because the output also yields $k_{diss,\infty}(T)$, the equilibrium constant was calculated from the appropriate values of the enthalpy and the structure and frequencies of *cis*- and *trans*-ClONO and $ClNO_2$, Cl, and NO_2 using the "Thermo" code in the Multiwell[4,5] suite, to compute the association rate constant, $k_{assn}(P,T)$. Table 2 shows values used in the calculations. Values of the equilibrium constant using critical energies from SM[7] are given in Table 3. (When other values of the critical energy were tried, the value of the equilibrium constant was recalculated. These are also shown in Table 3.)

"Hindered Gorin" Transition State. Using the value of the centrifugal maximum calculated above, the collision rate between Cl and NO_2 (taken as point particles) at 300 K would be in the range of 4 (ClONO)−6 ($ClNO_2$) × 10^{-10} cm^3 $molecules^{-1}$ s^{-1}, and this would be an upper limit for the high-pressure limit of the association rate constant. In the case of atom−radical associations, evidence suggests that the high-pressure limit approaches this upper limit. This is suggested by the values for the title processes in the NASA/JPL evaluation,[13] but the transition states in the SM[7] study yield a much lower value. As pointed out several times,[19] any tightening of the transition state can be modeled using the methods of variational transition state theory by changing frequencies of the transitional modes or by using a hindered Gorin transition state, which is tightened by restricting the rotations of the Cl and NO_2 reactants to less than the 4π steradians that could be available to them. Not much restriction is to be expected when one of the reactants is an atom. So, transition states for the barrierless association reactions were either taken directly from SM[7] or generated as above. Using the hindered Gorin model, values for the high-pressure limit rate constant for $ClNO_2$ and ClONO forming pathways turns out to be about 8×10^{-11} and 1×10^{-10} cm^3 $molecules^{-1}$ s^{-1}, respectively. (These values are smaller than the point particle values due to the finite size of the real species.) Stabilizing the ClONO species by 2 kcal mol^{-1} does not change this value. Increasing the *J* moment or using a Lennard−Jones potential raises the value. The Morse parameter in ZL[8] for ClONO has been adopted herein. They use slightly different thermochemistry from this work, and their high-pressure combination rate constants are about 6×10^{-11} cm^3 $molecules^{-1}$ s^{-1}. The difference is small with respect to the final low-pressure rate constant values, but small differences in the high-pressure limit do result.

Energy Transfer Parameters. The values for $\langle\Delta E\rangle_{down}$, the energy transfer parameter used in the exponential down model of energy transfer, and the Lennard−Jones collision diameters and well depths are given in Table 2. The Lennard−Jones parameters for nitrogen and the isomers of ClONO were taken from PG.[14] The initial value chosen for $\langle\Delta E\rangle_{down}$ was 300 cm^{-1}. This seemed "reasonable" based on experience but represents a fitting parameter that can make up for a gap in knowledge that includes the probability distribution function for energy transfer, the actual value, or values, of the energy transferred in a collision, and the lack of consideration of anharmonicity. A somewhat high value of 500 cm^{-1} was finally chosen. ($\langle\Delta E\rangle_{down}$ can be temperature-dependent; this kind of variation was not employed here. It is entirely conceivable that small

TABLE 1: Calculation of Centrifugal Maxima

By Maximizing $V(r) = De\{1 - \exp[-\beta(r - r_e)]\}^2 + kT(r_{max}/r)^2$	
$ClNO_2$	T (K) = 300
$Cl-NO_2$ stretching frequency	ω (cm^{-1}) = 371
bond energy	D_o (cm^{-1}) = 11150.2
change in zpe between $Cl + NO_2$ and $ClNO_2$	Δzpe (cm^{-1}) = 767.8
$D_o + \Delta$zpe	D_e (cm^{-1}) = 11918
mass of Cl	M_a (amu) = 35.5
mass of NO_2	M_b (amu) = 46
reduced mass	μ (amu) = 20.04
2D moment of inertia	J (amu Å^2) = 122.7
$Cl-NO_2$ bond length	r_e (Å) = 1.877
COM bond length = $(J/\mu)^{1/2}$	r_{ee} (Å) = 2.475
Morse $\beta = 0.12177\omega(\mu/D_e)^{1/2}$	β (Å^{-1}) = 1.852
r_{max} (center of mass)	r_{max} (Å) = 5.954
r_{max} (bond distance) = r_{max} (center of mass) − ($r_{ee} - r_e$)	r_{max} (Å) = 5.36
cis-ClONO	T (K) = 300
Cl−ONO stretching frequency	ω (cm^{-1}) = 618.2
bond energy	D_o (cm^{-1}) = 8016.4
change in zpe between $Cl + NO_2$ and *cis*-ClONO	Δzpe (cm^{-1}) = 261.8
$D_o + \Delta$zpe	D_e (cm^{-1}) = 8278.2
mass of Cl	M_a (amu) = 35.5
mass of NO_2	M_b (amu) = 46
reduced mass	μ (amu) = 20.04
2D moment of inertia	J (amu Å^2) = 129.6
Cl−ONO bond length	r_e (Å) = 1.774
COM bond length = $(J/\mu)^{1/2}$	r_{ee} (Å) = 2.543
Morse $\beta = 0.12177\omega(\mu/D_e)^{1/2}$ (Morse β from ZL = 2.71)	β (Å^{-1}) = 3.937
r_{max} (center of mass)	r_{max} (Å) = 4.19[4.86]
r_{max} (bond distance) = r_{max} (center of mass) − ($r_{ee} - r_e$)	r_{max} (Å) = 3.42[4.09]

By Maximizing $V(r) = D_e\{1 - \exp[\beta(r - r_e)]\}^2 + BJ(J + 1)/\mu r^2$

$ClNO_2$		T (K) = 300
r (A^{-1})	J	$E_0(J) - E_0(J = 0)$ (cm^{-1})
8.986	10	1.146
8.093	20	5.395
7.552	30	13.719
6.849	50	45.737
6.372	70	102.987
6.090	85	165.829
5.850	100	248.306
5.230	150	696.694
4.765	200	1489.628
4.037	300	4661.737
ClONO	using $\beta = 2.71$ from ZL	T (K) = 300
r (A^{-1})	J	$E_0(J) - E_0(J = 0)$ (cm^{-1})
6.673	10	2.078
6.074	20	9.578
5.713	30	23.974
5.246	50	77.958
4.931	70	171.974
4.745	85	273.163
4.588	100	403.694
4.186	150	1087.545
3.886	200	2239.742
3.419	300	6499.307

changes in some of the other fitting parameters would accommodate a temperature dependence for $\langle\Delta E\rangle_{down}$.)

3. Results and Discussion

The focus of this work has been to see if the data at 300 K can be fit using the data from recent quantum calculations. Figure 1 shows most of this data. Some caveats: The Leu data[1] were only taken at pressures up to 10 Torr (3×10^{17}), and the lines are extrapolations of the reported third-order rate constants. The data labeled Ravi He at 298 K-corrected to N_2 were plotted by multiplying the He pressures by 0.48 to bring them into agreement with the N_2 data. Although the N_2 data from Leu[1] and Ravishankara et al.[2] are in agreement, their He data differ by about 35%. The correction to the Seely et al.[3] Ar data was done by multiplying the Ar pressures by 0.5 to bring the lowest points into agreement with the N_2 data of Ravishankara et al.[2] Experience with other systems suggests that this factor of 2 difference between Ar and N_2 may be somewhat too great. The NASA Sum line is the result from the NASA/JPL evaluation[13] for the sum of values for the formation of ClONO (cis and trans were not differentiated) and $ClNO_2$. This latter curve implies that the data at the higher pressures show the effect of pressure falloff.

Using the values from SM,[7] together with the Lennard−Jones parameters in Table 2 and $\langle\Delta E\rangle_{down} = 500$ cm^{-1}, the computed values are shown by the red curves in Figure 2. It is no surprise

TABLE 2: Parameters for Multiwell Calculations

cis-ClONO	
critical energy at 0 K (kcal mol^{-1})	20.92 or 22.92 (see text)
vibrational frequencies (cm^{-1})	1731, 859, 618, 429, 245, 378
(*J*-rotor) adiabatic moments of inertia (AMU A^2)	129.6
(*K*-rotor) active external rotor (AMU A^2)	28.2
symmetry; electronic degeneracy; optical isomers	1; 1; 1
cis-Cl---ONO (Gorin Transition State) 300 K	
frequencies (cm^{-1})	750, 1318, 1618
(*J*-rotor) adiabatic moments of inertia (AMU A^2)	444.5
(*K*-rotor) active external rotor (AMU A^2)	27.8
moments of inertia active 2D rotor (AMU A^2)	11.1 (NO_2)
hindrance	0%
symmetry; electronic degeneracy; optical isomers	1; 1; 1
collisions: σ (A^2); ϵ (K)	
cis-ClONO	4.26; 336.4
N_2	3.61; 91.5
$\langle\Delta E\rangle_{down}$ (cm^{-1})	500
$ClNO_2$	
critical energy at 0 K (kcal mol^{-1})	31.88
vibrational frequencies (cm^{-1})	1801, 1342, 798, 639, 390, 345
(*J*-rotor) adiabatic moments of inertia (AMU A^2)	122.7
(*K*-rotor) active external rotor (AMU A^2)	38.7
symmetry; electronic degeneracy; optical isomers	2; 1; 1
Cl---NO_2 (Gorin Transition State) 300 K	
frequencies (cm^{-1})	750, 1318, 1618
(*J*-rotor) adiabatic moments of inertia (AMU A^2)	662.6
(*K*-rotor) active external rotor (AMU A^2)	38.3
moments of inertia active 2D rotor (AMU A^2)	9.34(NO_2)
hindrance	0%
symmetry; electronic degeneracy; optical isomers	2; 1; 1
collisions: σ (A^2); ϵ (K)	
$ClNO_2$	4.26; 336.4
N_2	3.61; 91.5
$\langle\Delta E\rangle_{down}$ (cm^{-1})	500
trans-ClONO	
critical energy at 0 K (kcal mol^{-1})	31.83
vibrational frequencies (cm^{-1})	1800, 852, 646, 403, 263, 173
(*J*-rotor) adiabatic moments of inertia (AMU A^2)	175.3
(*K*-rotor) active external rotor (AMU A^2)	10.2
symmetry; electronic degeneracy; optical isomers	1; 1; 1
trans-Cl---ONO (Gorin Transition State)	
frequencies (cm^{-1})	750, 1318, 1618
(*J*-rotor) adiabatic moments of inertia (AMU A^2)	149.8
(*K*-rotor) active external rotor (AMU A^2)	25.1
symmetry; electronic degeneracy; optical isomers	1; 1; 1
collisions: σ (A^2); ϵ (K)	
$ClNO_2$	4.26; 336.4
N_2	3.61; 91.5
$\langle\Delta E\rangle_{down}$ (cm^{-1})	500
cis−trans Isomerization Transition State	
critical energy at 0 K (kcal mol^{-1})	8.75
frequencies (cm^{-1})	1752, 1339, 789, 405,222
(*J*-rotor) adiabatic moments of inertia (AMU A^2)	377.1
(*K*-rotor) active external rotor (AMU A^2)	5.57
symmetry; electronic degeneracy; optical isomers	1; 1; 1

TABLE 3: Equilibrium Constants (Molecules/cm^3)

T (K)	Cl + NO_2 ↔ $ClNO_2$	Cl + NO_2 ↔ *cis*-ClONO	Cl + NO_2 ↔ *trans*-ClNO
300 SM heats[a]	4.77×10^{-3}	1.21×10^{-10}	7.47×10^{-13}
200 SM heats	2.77×10^{9}	6.17×10^{-3}	2.46×10^{-6}
300 stabilized[b]		3.46×10^{-9}	2.14×10^{-11}
200 stabilized		9.45×10^{-1}	3.77×10^{-4}

[a] Using ΔH from SM.[7] [b] Stabilizing *cis*-ClONO and *trans*-ClONO by 2 kcal mol^{-1}.

that the high-pressure limits are much lower than the NASA/JPL values, as the transition states are quite "tight".

Using the structures and other parameters from ZL,[8] including the formation of *trans*-ClONO without a barrier, in a calculation as described above, a similar problem is found. The $ClNO_2$ production is about the same as the Gorin calculation in Figure 2, and the ClONO production is about 50% higher. In their own calculations, ZL apparently have no such difficulty.

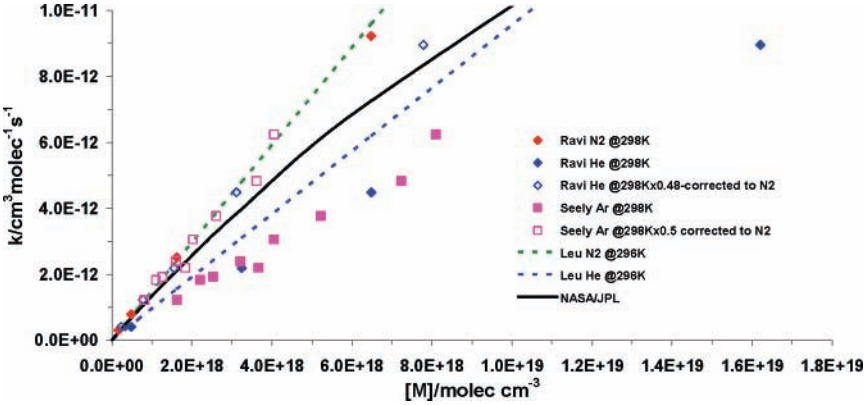

Figure 1. Data at 298 K from Leu,[1] Ravishankara et al.,[2] and Seely et al.[3] and the value from the NASA/JPL evaluation.[13] Measured data are depicted with solid symbols. Open symbols are corrected to N_2 as the bath gas.

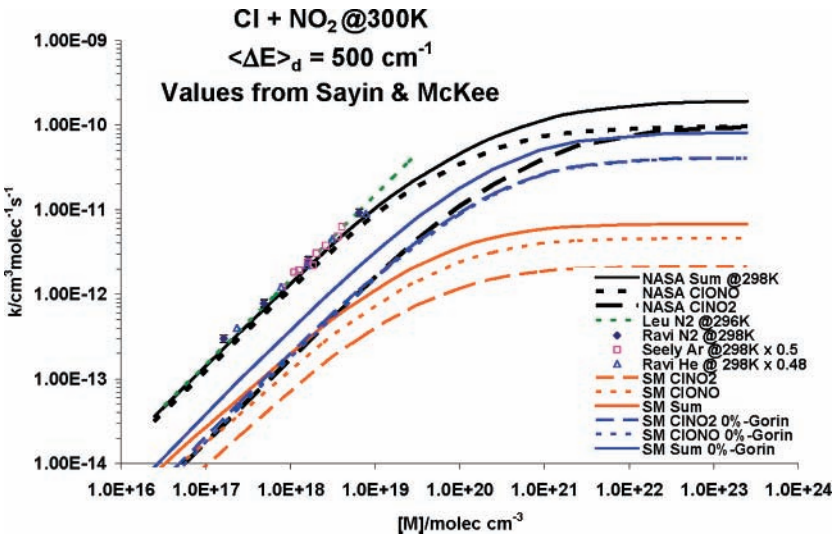

Figure 2. Data from Figure 1 together with values (black curves) from the NASA/JPL evaluation[13] for ClONO and $ClNO_2$ production, as well as the sum of these. Similar curves were computed with "Multiwell" for the values from SM[7] with $\langle \Delta E_d \rangle = 500$ cm^{-1} (red curves) and using a 0%-hindered Gorin model using energies from SM[7] (i.e., a substantial barrier to direct formation of *trans*-ClONO) (blue curves).

They used a combination of the codes ChemRate[20] and Variflex,[21] and a repetition of their computations would be difficult to carry out absent many input variables.

To test the effect of changing the transition states for chlorine atom association with nitrogen dioxide, these were taken as Gorin transition states as described earlier. The results are as shown by the blue curves in Figure 2. Although the transition states are all Gorin type, the barrier to *trans*-ClONO formation was kept at the value in SM.[7] Because the cis−trans isomerization barrier is low, *trans*-ClONO is still formed by that route. The reduction of this barrier to zero has a small effect on the high-pressure limit values but does not affect the low-pressure values. Notice that although experiment[9] seems to suggest that the ClONO species should be formed at 3−4 times the rate for $ClNO_2$, the results in Figure 2 from the Gorin calculations do not show this, whereas those in Figure 2 computed with the tighter transition states do support a higher value for ClONO formation by a factor of about two.

As a way of enhancing the ratio of ClONO to $ClNO_2$ formation, the stability of the ClONO isomers was enhanced by 2 kcal mol^{-1}, which would seem to be within the uncertainty in the calculated stabilities. The value of $\langle \Delta E_d \rangle$ used was 500 cm^{-1}. The results are shown as the red lines in comparison to the data in Figure 3.

The results shown in Figure 3 may indicate that the computed density of states is not high enough to match the data. Anharmonicity effects might be as high as a factor of 2, but this is difficult to estimate. Another way to increase the state density would be to include all external rotations as active. The results of this change are shown in Figure 4. Apparently this change is sufficient to fit the data. Although, the total curve is about a factor of 1.5 lower at the high-pressure end and also displays signs of falloff behavior not necessarily apparent in the data.

Although the inclusion of all rotations as active fits the data, it is not the only way that this can be accomplished. Although it is common to use the Lennard−Jones collision frequency in three types of calculations, it is not entirely clear that either this is the correct formula or the cross-section and well depth are well-known for molecules of this type. As an exercise, one can increase these latter values in an attempt at fitting the data. Figure 5 shows the results of increasing the cross-section for both ClONO and $ClNO_2$ from 4.26 to 7.00 A and the well depth from 336.4 to 1000 cm^{-1}.

It is not the purpose of this exercise to suggest that either of the changes shown in Figures 4 or 5 are correct. Clearly some combination, including anharmonicity, would yield similar results.

Calculations using the stabilized ClONO and $\langle \Delta E_d \rangle$ of 500 cm^{-1} at 200 K suggest a temperature dependence of the low-pressure limit rate constant of about $T^{-1.8}$. Leu[1] reports a

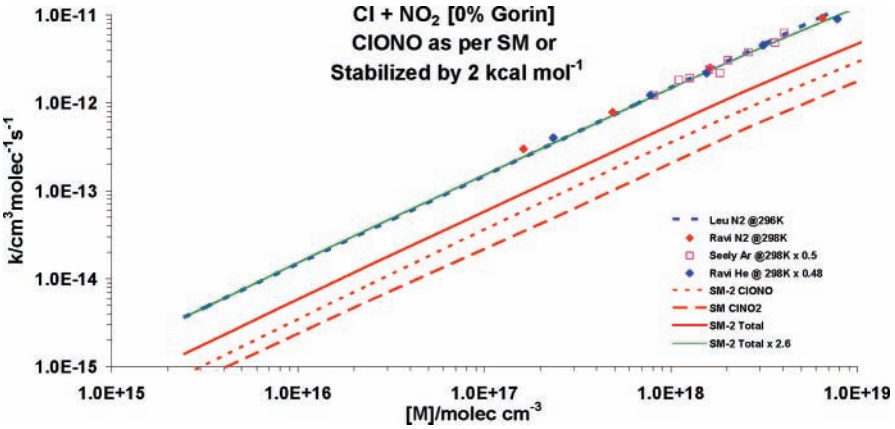

Figure 3. Similar to Figure 2 but showing only the pressure range where data exist. Red curves are computed with both the isomers of ClONO and the isomerization transition state stabilized by 2 kcal mol^{-1}. $\langle \Delta E_d \rangle = 500$ cm^{-1} for all curves in this figure. The $ClNO_2$ curve is unaffected by the change in stability of ClONO. The green line is the solid red line multiplied arbitrarily by 2.6 to fit the data.

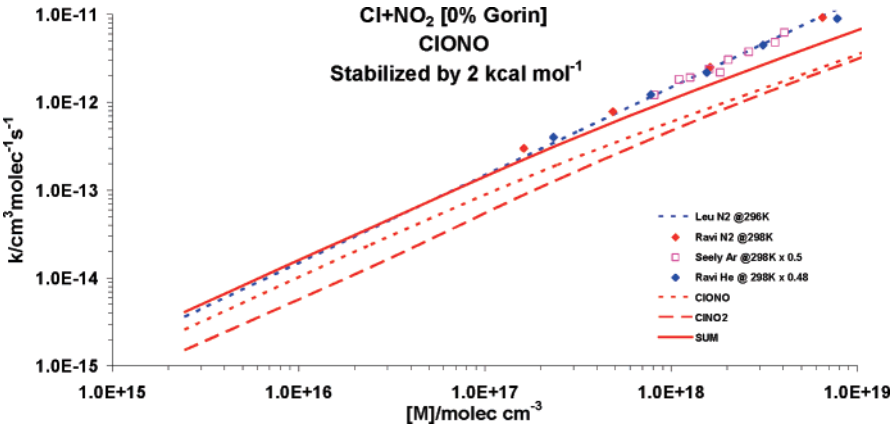

Figure 4. Exactly as the red lines in Figure 3, except that all external rotations are treated as active.

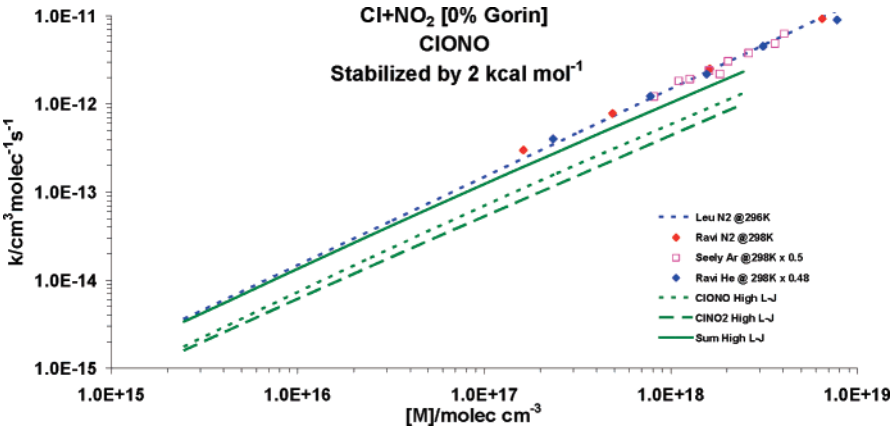

Figure 5. Exactly as the red lines in Figure 3, except that the Lennard−Jones collision frequency has been increased from 3.5×10^{-10} to 7.7×10^{-10}.

value of $T^{-2.0\pm0.5}$ in He for [264 < T (K) < 417], and PG[14] compute a similar value.

4. Application of the Troe Model

PG[14] applied the Troe model[11] described in 1977 and updated it in 1979[12] to both pathways. (They did not distinguish between *cis*- and *trans*-ClONO.) They found that a value of $\beta_c = 0.28$ describes the data for each product channel. More recent values of some of the input parameters change the result. In particular, PG used a value of 108 cm^{-1} for the torsional frequency that appears to be too low. This has a substantial effect on the results. As discussed in the Appendix, the application of the Troe formalism gives the same results as the calculations discussed above. In each case, the data are not explained without including effects that are not specifically included in either method.

5. $ClNO_2$ Decomposition

Hiraoka and Hardwick (HH)[22] and Cordes and Johnston (CJ)[23] have studied the thermal decomposition of $ClNO_2$. HH[22] report data in Ar between 678 and 1032 K at molecular densities

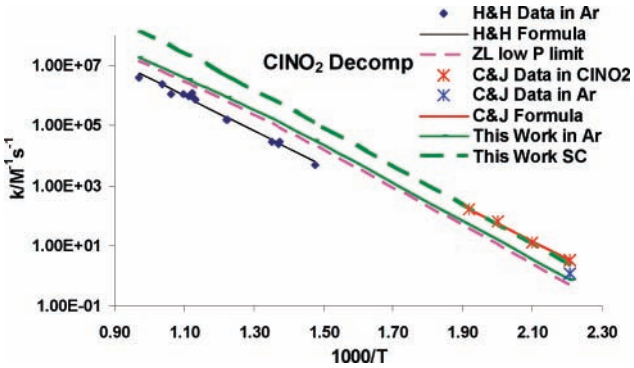

Figure 6. Second-order rate coefficients for the decomposition of $ClNO_2$. Data and fits from HH[22] and CJ.[23] Computations from ZL[8] and this work.

ranging from 7.5×10^{18} at the lowest temperature to 4.2×10^{18} molecules cm^{-3} at the highest temperature. CJ[23] report data in pure $ClNO_2$ at temperatures between 453 and 521 K. They report second-order rate constants directly. They also performed experiments in Ar at only 453 K with molecular densities in the range of 1.2×10^{17} to 1.5×10^{18} molecules cm^{-3}. They extracted a second-order rate constant from the data at densities up to about 3×10.[17]

ZL[8] take note of these studies and report an expression for the decomposition at 10^{-4} Torr, which should represent essentially the low-pressure limit. Calculations using the parameters that produced the pink lines in Figure 3, namely, the 0% Gorin transition state with only the "*K*-rotor" taken as active and with thermochemical parameters based on SM,[7] yield values in agreement with the ZL[8] expression. Data and calculations are shown in Figure 6. Interestingly, this result is slightly higher than the HH data, so if these data are taken at face value and the parameters for $ClNO_2$ are adjusted to comply, computations of the type shown in Figure 3 would be further from the data shown in that figure. On the other hand, the CJ data are higher than the calculation in keeping with the observation at 300 K. (To compute values for the CJ data in pure $ClNO_2$, the Lennard−Jones collision rate would be slightly lower when taking like−like collisions into account and the value of $\langle \Delta E_{down} \rangle$ might be larger, so about the same value as the Ar calculation might be expected.)

6. Conclusions

The most significant conclusion, which is not new, is that the most uncertain part of knowledge for pressure-dependent unimolecular and association reactions is in the low-pressure limit. Effects due to accurate values of heats of formation, probability distribution and amounts of energy transferred, the interaction of rotation and vibration, and anharmonicity all play a role. Note should also be taken of the fact that the data are not without some uncertainty. So for reactions close to the low-pressure limit, extrapolation out of the experimental range would seem to be subject to large uncertainties.

Additionally, as shown in detail in the Appendix, codes such as Multiwell give the same results as the Troe formalism, when the disposition of rotational density is considered correctly.

Acknowledgment. This work was supported through Grant #NNG06GF98G "Critical Evaluation of Kinetic Data/Applied Theory" from The NASA Upper Atmosphere Research Program. Discussions with John Barker, Jürgen Troe, and Gregory Smith were extremely useful. Professor Michael McKee, Auburn University, was kind enough to send unpublished details of his work.

Appendix: Reconciliation of Troe Method with "RRKM" Method for Calculation of Low-Pressure Rate Constants

Troe[11,12] developed a formalism for computing low-pressure rate constants in a masterful set of expositions three decades ago. He suggested that the low-pressure rate constant could be calculated by first calculating the value for a purely harmonic case, ignoring the effect of angular momentum conservation, anharmonicity, the energy dependence of the density of states, and any correction for internal rotation. He then developed a set of correction factors to account for each of these effects.

Using Barker's "Multiwell" code, which employs methods found in textbooks, one can also calculate the low-pressure limiting rate constant and comparisons may be made.

For purposes of this discussion, the dissociation of the molecule $ClNO_2$ at 300 K is examined. (Of course, this dissociation would be very slow, but multiplication by the equilibrium constant will allow a consideration of the association of Cl with NO_2 to yield $ClNO_2$.)

Troe gives

$$k_0^{sc}/[M] = Z_{LJ}[\rho_{vib,h}(E_0)kT/Q_{vib}] \times F_{anh}F_E F_{rot}F_{rotint}F_{corr} \quad \text{(A1a)}$$

where Z_{LJ} is the Lennard−Jones collision rate, $\rho(E_0)$ is the harmonic density of states at the critical energy, and the F values are correction factors for the effect on the density of states of anharmonicity, energy dependence, angular momentum conservation, and anything else.

In the current exercise, only harmonic frequencies are employed and there is no internal rotation. F_{corr} is taken to be unity. The most important correction concerns the effect of angular momentum conservation, F_{rot}.

Troe addresses this by first computing the maximum correction, which would hold if only $J = 0$ were allowed; thus, there would be no centrifugal barriers. In this case, all of the rotational energy of the molecule would be available for the reaction. This is given by:

$$F_{rotmax} = (1/Q_{rot})[\rho_{rovib,h}(E_0)/\rho_{vib,h}(E_0)] \quad \text{(A2)}$$

where $\rho_{rovib,h}(E_0)$ is the harmonic density of states including rotations.

Two formulations are given for F_{rotmax}, one for a linear molecule and one for a nonlinear molecule.

$$F_{rot,max}^{linear} \equiv F_{rot,J,max} \approx \frac{1}{s}\left[\frac{E_0 + a(E_0)E_z}{kT}\right] \quad \text{(A3a)}$$

and

$$F_{rot,max}^{nonlinear} \approx \frac{(s-1)!}{(s+1/2)!}\left[\frac{E_0 + a(E_0)E_z}{kT}\right]^{3/2} \quad \text{(A3b)}$$

where s is the number of oscillators, $a(E_0)$ is the Whitten−Rabinovitch[24] correction factor, and E_z is the zero-point energy.

F_{rot} is computed from a small variation of a formula proposed by Waage and Rabinovitch.[25] For linear molecules

$$F_{rot}^{linear} = F_{rot,max}^{linear}\frac{\bar{I}/I}{\bar{I}/I - 1 + F_{rot,max}^{linear}} \quad \text{(A4a)}$$

and for nonlinear molecules

$$F_{\text{rot}}^{\text{nonlinear}} = F_{\text{rot},K} \times F_{\text{rot},J} = F_{\text{rot,max}}^{\text{nonlinear}} \frac{I^{\neq}/I}{I^{\neq}/I - 1 + F_{\text{rot,max}}^{\text{nonlinear}}} \quad \text{(A4b)}$$

For linear molecules:

$$\frac{I^{\neq}}{I} = \frac{1}{Q_{\text{rot}}} \int_0^{\infty} \mathrm{d}J(2J+1)\exp\left[-\frac{E_0(J) - E_0(J=0)}{kT}\right] \quad \text{(A5a)}$$

For nonlinear molecules:

$$\frac{I^{\neq}}{I} = \frac{1}{Q'_{\text{rot}}} \int_0^{\infty} \mathrm{d}J(2J+1)2J\exp\left[-\frac{E_0(J) - E_0(J=0)}{kT}\right] \quad \text{(A5b)}$$

The $E_0(J)$ values are the centrifugal barriers, and the "prime" on the rotational partition function indicates that it is for a nonlinear molecule.

Application to $ClNO_2$. *Using the Nonlinear Formulation.* Treating $ClNO_2$ like the nonlinear molecule that it is, taking E_0 = 11150 cm^{-1}, using frequencies from SM,[7] and making use of the "Densum" code, which is part of the Multiwell suite, the value $\rho_{\text{vib,h}}(11150\ \text{cm}^{-1}) = 25.2\ \text{cm}^{-1}$ is obtained. Using collision parameters that yield Z_{LJ} (cm^3 $molecule^{-1}$ s^{-1}) = 3.50 × 10^{-10}, and the SM frequencies that yield Q_{vib} = 1.5, substituting into eq A1 and ignoring all but energy dependence of the density and rotational effects leads to:

$$k_0^{\text{sc}}/[\text{M}] = Z_{\text{LJ}}[\rho_{\text{vib,h}}(E_0)kT/Q_{\text{vib}}] \times F_{\text{E}}F'_{\text{rot}} \quad \text{(A6a)}$$

$$k_0^{\text{sc}}/[\text{M}] = 6.4 \times 10^{-30} \times F_{\text{E}}F'_{\text{rot}} \quad \text{(A7a)}$$

Using $s = 6$, $a(E_0) = 0.965$, E_z (cm^{-1}) = 2660, with E_0 (cm^{-1}) = 11150 and kT (cm^{-1}) = 208, and F'_{rotmax} = 34.3 for this nonlinear example.

F'_{rotmax} may also be computed from

$$F'_{\text{rotmax}} = (1/Q_{\text{rot}}')[\rho_{\text{rovib,h}}(E_0)/\rho_{\text{vib,h}}(E_0)] \quad \text{(A8a)}$$

where $\rho_{\text{rovib,h}}(E_0)$ is the harmonic density of states including rotations.

With $\rho_{\text{vib,h}}(11150\ \text{cm}^{-1}) = 25.2\ \text{cm}^{-1}$, $\rho_{\text{rovib,h}}(11150\ \text{cm}^{-1}) = 4.89 \times 10^7\ \text{cm}^{-1}$, and $Q'_{\text{rot}} = 5.76 \times 10^4$ (uncorrected for symmetry as proscribed by Troe), $F'_{\text{rotmax}} = 33.7$, in very good agreement with the above value of $F'_{\text{rotmax}} = 34.3$.

The $E_0(J)$ values were computed for a Morse potential, with a Morse β value of 1.852 A^{-1}. This value can be obtained from the force constant given by Lee. Computing the integral eq A5b for the nonlinear case above and with a value of $Q'_{\text{rot}} = 5.76 \times 10^4$ yields $I^{\neq}/I$ = 20.9, and thus, F'_{rot} = 13.1. A separate calculation of F_{E} yields 1.08, so that $k_0/[\text{M}]$ (cm^3 $molecules^{-1}$ s^{-1}) = 9.1 × 10^{-29}.

Using the Linear Formulation. Troe's formalism can also be used in a reformulated way if the calculation of $\rho_{\text{vib,h}}(E_0)$ is expanded to include the energy levels of the rotation along the figure axis, the "*K*-rotor". We can call this $\rho_{\text{vib}-K,\text{h}}(E_0)$. Now, eq A1a becomes

$$k_0^{\text{sc}}/[\text{M}] = Z_{\text{LJ}}[\rho_{\text{vib}-K,\text{h}}(E_0)kT/Q_{\text{vib}-K}] \times F_{\text{anh}}F_{\text{E}}F_{\text{rot}}F_{\text{rotint}}F_{\text{corr}} \quad \text{(A1b)}$$

$Q_{\text{vib}-K} = Q_{\text{vib}}(\Pi kT/A)^{1/2}$ includes the one-dimensional *K*-rotor, and F_{rot} will be for the linear case.

Taking E_0 = 11150 cm^{-1}, using frequencies from SM, and making use of the "Densum" code again, the value $\rho_{\text{vib}-K,\text{h}}(11150\ \text{cm}^{-1}) = 3.2 \times 10^3\ \text{cm}^{-1}$. Once more, using collision parameters that yield Z_{LJ} (cm^3 $molecule^{-1}$ s^{-1}) = 3.50 × 10^{-10}, and SM frequencies along with the value of $A = 0.436$ that yield $Q_{\text{vib}-K}$ = 58.1, leads to:

$$k_0^{\text{sc}}/[\text{M}] = Z_{\text{LJ}}[\rho_{\text{vib,h}}(E_0)kT/Q_{\text{vib}}] \times F_{\text{E}}F_{\text{rot}} \quad \text{(A6b)}$$

$$k_0^{\text{sc}}/[\text{M}] = 2.1 \times 10^{-29} \times F_{\text{E}}F_{\text{rot}} \quad \text{(A7b)}$$

Using $s = 6$, $a(E_0) = 0.965$, E_z (cm^{-1}) = 2660, with E_0 (cm^{-1}) = 11150 and kT (cm^{-1}) = 208, F_{rotmax} = 11.0.

F_{rotmax} may also be computed from

$$F_{\text{rotmax}} = (1/Q_{\text{rot}})[\rho_{\text{rovib,h}}(\text{E}_0)/\rho_{\text{vib}-K,\text{h}}(E_0)] \quad \text{(A8b)}$$

where $\rho_{\text{rovib,h}}(E_0)$ is the harmonic density of states including rotations and $\rho_{\text{vib}-K,\text{h}}(E_0)$ is the harmonic density of states including just the *K*-rotor.

With $\rho_{\text{rovib,h}}(11150\ \text{cm}^{-1}) = 4.89 \times 10^7\ (\text{cm}^{-1})$, $\rho_{\text{rovib}-K,\text{h}}(11150\ \text{cm}^{-1}) = 3.21 \times 10^3\ (\text{cm}^{-1})$, and $Q_{\text{rot}} = 1.51 \times 10^3$ (uncorrected for symmetry as proscribed by Troe), F_{rotmax} = 10.1, in very good agreement with the above value of F_{rotmax} = 11.0.

As in the nonlinear case, the $E_0(J)$ values were computed for a Morse potential, with a Morse β value of 1.852 A^{-1}. Computing the integral eq A5a for the linear case and with the value of $Q_{\text{rot}} = 1.51 \times 10^3$, yields $I^{\neq}/I$ = 5.4; thus, F_{rot} = 3.86. Using F_{E} = 1.08, $(k_0/[\text{M}])/\text{cm}^3\ \text{molecules}^{-1}\ \text{s}^{-1} = 8.8 \times 10^{-29}$ in almost exact agreement with the nonlinear result of $(k_0/[\text{M}])/\text{cm}^3\ \text{molecules}^{-1}\ \text{s}^{-1} = 9.1 \times 10^{-29}$! (It is also interesting to note that if $I^{\neq}/I$ is computed by assuming that the value of rotational energy at the maximum is kT, the value 5.45 results.)

Comparison with Multiwell. In using the Multiwell suite, the "*K*-rotor" is typically included in the density calculation. Using the same input data, the Multiwell suite yields $(k_0/[\text{M}])/\text{cm}^3\ \text{molecules}^{-1}\ \text{s}^{-1} = 9.5 \times 10^{-29}$. This is reasonable agreement and may be thought of as a value of F_{rot} = 4.19.

Therefore, it is clear that the Troe formalism gives the same result as the Multiwell code, which uses more direct methods to calculate the state density and which also incorporates pressure dependence directly.

References and Notes

(1) Leu, M. T. *Int. J. Chem. Kinet.* **1984**, *16*, 1311.

(2) Ravishankara, A. R.; Smith, G. J.; Davis, D. D. *Int. J. Chem. Kinet.* **1988**, *20*, 811.

(3) Seeley, J. V.; Jayne, J. T.; Molina, M. J. *J. Phys. Chem.* **1996**, *100*, 4019.

(4) Barker, J. R. *Int. J. Chem. Kinet.* **2001**, *33*, 232−245.

(5) Barker, J. R. *MultiWell-2.08 Software*;Ortiz, N. F., Preses, J. M., Lohr, L. L., Maranzana, A., Stimac, P. J., contibutors; University of Michigan: Ann Arbor, MI, 2007; http://aoss.engin.umich.edu/multiwell/.

(6) Lee, T. J. *J. Phys. Chem.* **1994**, *98*, 111.

(7) Sayin, H.; McKee, M. L. *J. Phys. Chem. A* **2005**, *109*, 4736−4743.

(8) Zhu, R. S.; Lin, M. C. *Chemphyschem* **2004**, *5*, 1864.

(9) Niki, H.; Maker, P. D.; Savage, C. M.; Breitenbach, L. P. *Chem. Phys. Lett.* **1978**, *59*, 78.

(10) Chang, J. S.; Baldwin, A. C.; Golden, D. M. *J. Chem. Phys.* **1979**, *71*, 2021.

(11) Troe, J. *J. Chem. Phys.* **1977**, *66*, 4758.

(12) Troe, J. *J. Phys. Chem.* **1979**, *83*, 114−126.

(13) Sander, S. P.; Friedl, R. R.; Golden, D. M.; Huie, R. E.; Kolb, C. E.; Kurylo, M. J.; Molina, M. J.; Moortgat, G. K.; Orkin, V. L.; Ravishankara, A. R.; Wine, P. H. *Chemical Kinetics and Photochemical Data for Use in Atmospheric Studies, Evaluation Number 15*; Jet Propulsion Laboratory: 2006.

(14) Patrick, R.; Golden, D. M. *Int. J. Chem. Kinet.* **1983**, *15*, 1189−1227.
(15) Holbrook, K. A.; Pilling, M. J.; Robertson, S. H. *Unimolecular Reactions*, 2 ed.; Wiley: Chichester, 1996.
(16) Golden, D. M. *J. Phys. Chem. A* **2006**, *110*, 2940−2943.
(17) Walsh, R.; Golden, D. M. **2006**, unpublished.
(18) Golden, D. M. *Int. J. Chem. Kinet.* **2007**, to be submitted.
(19) Golden, D. M.; Barker, J. R.; Lohr, L. L. *J. Phys. Chem.* **2003**, *107*, 11057−11071.
(20) Mokrushin, V.; Bedanov, V.; Tsang, W.; Knyasev, V. D. *ChemRate*, Version 1.19; 2002. http://www.nist.gov/kinetics/chemrate/chemrate.html.
(21) Klippenstein, S. J.; Wagner, A. F.; Dunbar, R. C.; Wardlaw, D. M.; Robertson, S. H. *VARIFLEX*, Version 1.00; http://chemistry.anl.gov/chem-dyn/VariFlex/index.html, 1999.
(22) Hiraoka, H.; Hardwick, R. *J. Chem. Phys.* **1962**, *36*, 2164.
(23) Cordes, H. F.; Johnston, H. S. *J. Am. Chem. Soc.* **1954**, *76*, 4264.
(24) Whitten, G. Z.; Rabinovitch, B. S. *J. Chem. Phys.* **1963**, *38*, 2466.
(25) Waage, E. V.; Rabinovitch, B. S. *Chem. Rev.* **1970**, *70*, 377.